DOI 10.1007/s11106-023-00344-x
Powder Metallurgy and Metal Ceramics, Vol. 61, Nos. 9-10, January, 2023 (Russian Original Vol. 61, Nos. 9-10, Sept.-Oct., 2022)

SINTERING OF FERROMAGNETIC MATERIALS AT LOWER TEMPERATURES IN HYDROGEN

I. Sm_2Co_{17} ALLOYS

I.I. Bulyk[1,2,3] and O.P. Kononiuk[1]

UDC 669/661.8/536.4/620.3

Scanning electron microscopy and X-ray energy-dispersive spectroscopy were employed to study the sintering of powders from the induction-melted industrial ferromagnetic $Sm_2(Co,Fe,Zr,Cu)_{17}$ alloy by the hydrogenation, disproportionation (HD), desorption, recombination (DR) (HDDR) route. The HD stage proceeded at 700°C and DR at 950°C. The experimental results showed that sintering of the powders occurred at the HD stage to produce a mechanically integral highly porous material. The porosity of the sintered materials was found to decrease as the compaction pressure and powder particle refinement increased. The powder compaction pressure was estimated to range from 2 to 5 t/cm^2. The decrease in sintering temperature was attributed to the higher diffusion rate of the alloy components resulting from the decrease in particle size, hydrogen-initiated phase transformations, and the hydrogen solid solution present in the alloy. Phase transformations occurred when the pressure changed at high temperatures. If the hydrogen pressure was high, the intermetallic was not thermodynamically stable and disintegrated (disproportionated) into several phases. If the hydrogen pressure was low (vacuum), the rare earth metal hydride was thermodynamically unstable and disintegrated, while the rare earth metal interacted with other phases to form the starting intermetallic. These phenomena are due to chemical reactions within a solid body, proceeding through the diffusion of components. The new sintering method for ferromagnetic materials has process advantages over existing methods: it does not require holding at the highest heating temperatures or usage of complex dies or complex equipment and results in the production of anisotropic nanostructured materials. Ways to improve the properties of sintered materials at low temperatures (in particular, increasing the homogeneity of their microstructure and decreasing the porosity) are proposed, such as optimization of sintering parameters and homogenization of the powders by particle size.

Keywords: *hydrogenation, disproportionation, desorption, recombination, samarium–cobalt ferromagnetic materials, sintering, phase transformations, microstructure.*

[1]Karpenko Physicomechanical Institute, National Academy of Sciences of Ukraine, Lviv, Ukraine. [2]Institute for Rare Earth Magnetic Materials and Devices (IREMMD), Jiangxi University of Science and Technology, Ganzhou, China.

[3]To whom correspondence should be addressed; e-mail: i.bulyk@jxust.edu.cn.

Translated from Poroshkova Metallurgiya, Vol. 61, Nos. 9–10 (547), pp. 76–90, 2022. Original article submitted July 18, 2022.

INTRODUCTION

Permanent magnets, particularly those produced from rare earth and transition metal compounds (REM-TM)—$Nd_2Fe_{14}B$, $SmCo_5$, and Sm_2Co_{17}—are components in many devices that have become indispensable to modern life, including wind generators, hybrid and electric cars, household appliances, computer hard drives, etc. [1]. In recent decades, the application of permanent magnets has expanded significantly, primarily because of the rapid increase in the production of electric vehicles and wind power generators [2]. Magnets based on $Nd_2Fe_{14}B$ have the highest residual induction and magnetic energy [3], but their temperature range of application is relatively narrow, not exceeding 200°C [4]. For operating temperatures between 250 and 550°C, samarium–cobalt materials are used [4]. Although the usage of these magnets is relatively low [5], they are indispensable in devices such as accelerometers and gyroscopes, high-efficiency motors and generators, high-temperature magnetic bearings (including those for aircraft engines), magnetic clutches and starters, high-efficiency pumps and mixers, waveguides, ion engines for space vehicles, surgical instruments, etc. [6].

Nanocomposites will usher the next generation of magnets: ferromagnetic materials comprising a mixture of nanostructured magnetically soft and hard phases [7]. They will show improved properties compared to microcrystalline materials, such as higher residual magnetization and greater magnetic energy, resulting from the exchange interaction between the two nanostructured ferromagnetic phases [8, 9].

New processing methods for ferromagnetic materials are required to refine the microstructure to the nanoscale and produce sintered magnets. The microstructure refinement is relatively simple to achieve. For this purpose, spinning, high-energy mechanical grinding, chemical reactions etc. are particularly employed [10]. However, ingenious approaches are needed to produce solid (sintered) materials because conventional sintering methods require high temperatures. In this case, the microstructure consists of microsized grains. The methods for producing nanostructured magnetic materials are developed in several areas. Hence, alloys are ground into powders with 9–16 nm particles [11]. Nevertheless, a significant portion of samarium tends to oxidize in such powders.

Spark plasma sintering (SPS) is a method for sintering nanostructured magnets. The single-phase Sm_2Co_{17} alloy is first subjected to high-energy grinding to become amorphous and then to SPS to sinter and become nanostructured [12]. Although the magnetic properties of the sintered materials are low, the authors propose that this method is used as a basis for further improvement.

The same approach was applied to $SmCo_{6.6}Ti_{0.4}$ [13] and '$SmCo_7$'[1] materials [14]. Anisotropic polycrystalline lamellae approximately 200 nm thick and up to 20 μm long were produced by grinding. The powder was sintered through SPS to form a partially textured nanostructured magnetic with a hysteresis loop rectangularity of 0.8 and grain sizes of 36–38 nm [13]. The influence of heat treatment conditions following SPS on the phase composition, microstructure, and magnetic properties of the sintered materials was studied in [14]. The SPS method proved to be successful for sintering high-density nanostructured ferromagnetic materials. The method is disadvantageous in that the materials have low texture.

Many researchers are studying the potential of using hot pressing and deformation to produce compact nanostructured magnets. For instance, the researchers [15] ground the $Sm(Co_{0.58}Fe_{0.31}Zr_{0.05}Cu_{0.04}B_{0.02})_z$ spinning alloy (z = 7.5–12) and pressed it at 750°C for 30 sec under 172 MPa and then deformed it at 900°C for 3–5 min under 35–55 MPa. The samples showed partial anisotropy after the deformation. The alloy with z = 10 achieved the highest magnetic energy: $(BH)_{max}$ = 10.6 MGOe.

Anisotropy is a necessary condition for imparting high properties to magnets produced from REM-TM alloys. To develop anisotropy in samarium–cobalt alloys of various composition, they were processed by SPS and hot deformation [16]. The researchers found that Sm_2Co_{17} alloys could not be textured through this processing,

[1]The $SmCo_7$ phase is quasistable, and part of cobalt is replaced by other metals to stabilize this phase. In the literature, this phase is denoted as $SmCo_7$ and '$SmCo_7$', indicating that it includes other metals instead of cobalt. We used the second notation.

while $SmCo_5$, Sm_2Co_7, and disordered Sm_2Co_{17} ('$SmCo_7$') did acquire texture. The tendency to acquire texture through hot deformation increases in the following order: Sm_2Co_{17}(R) < '$SmCo_7$' < $SmCo_5$ < Sm_2Co_7.

The paper [17] studied the effect of strain on the texture and magnetic properties of REM–cobalt alloys. High properties of the $SmCo_5$ alloy are achieved by increasing the strain to 94.5%: H_c = 22.8 kOe and $(BH)_{max}$ = = 18.0 MGOe. The alloy microstructure was refined to 100–500 nm grains through deformation.

Therefore, the current nanostructuring methods are not sufficient for creating magnets with enhanced properties because they have low texture. We propose a different approach to solve the issue, which is to use hydrogen treatment to refine ferromagnetic materials to the nanoscale and sinter them. Anisotropic ferromagnetic materials are also produced by this method.

The objective of this research is to demonstrate the potential of hydrogen treatment through the hydrogenation, disproportionation (HD), desorption, and recombination (DR) (HDDR) route for sintering $Sm_2(Co,Fe,Zr,Cu)_{17}$ alloys at low temperatures and to evaluate the effect of powder grinding conditions, compaction pressure, and sintering stages (HD and HDDR) on the microstructure of the sintered materials.

METHODOLOGY

The induction-melted industrial ferromagnetic $Sm_2(Co,Fe,Cu,Zr)_{17}$ alloy, designated as KS25 (Fig. 1), was studied. The alloy samples were hydrogenated and ground in water using a Pulverisette 6 single-chamber planetary-ball mill. The grinding time (τ) was 20 and 60 min at a chamber rotation frequency (ν) of 100 rpm and 60 min at ν = 200 rpm. The powders were then compacted at pressures of 2, 5, and 20 t/cm^2.

The compacts were sintered in both hydrogen and vacuum through HD at a hydrogen pressure up to 1.5 MPa and a temperature of 700°C and through HDDR at a resorption and recombination temperature of 950°C.

X-ray diffraction (XRD) analysis was performed using the diffraction patterns produced with a DRON-2.0 diffractometer (Fe-K_α radiation). The PowderCell software was used to identify the phases [18]. The lattice parameters of the phases were determined with the FullProf software [19].

A JSM-6490 (JEOL) electron scanning microscope equipped with an INCA ENERGY 350 energy-dispersive X-ray spectrometer was employed to study the morphology of the powders and sintered alloys. The powders were applied onto a conductive adhesive tape. To examine the microstructure of particles, the powder was embedded in conductive cement, while the sintered materials were embedded in Wood's metal. The samples were subsequently ground and polished with diamond pastes with varying abrasive particle sizes. The materials were studied in polished and etched states. For the etching process, a solution comprising 5 vol.% nitric acid and ethanol was used. The etching time was no more than 60 sec.

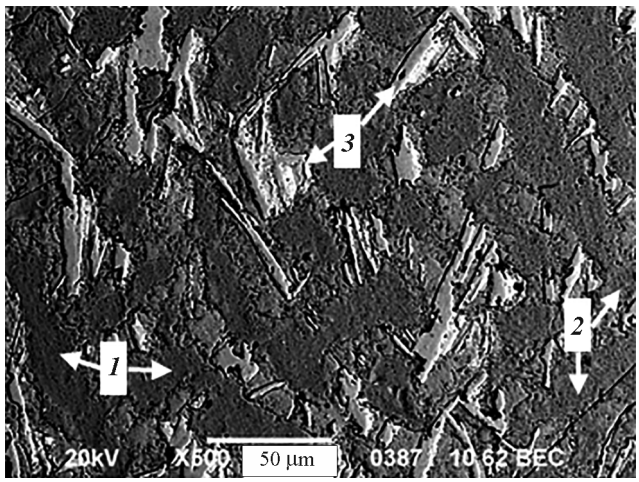

Fig. 1. Microstructure of the starting KS25 alloy: *1*) $Sm_2(Co,Fe,Zr,Cu)_{17}$ phase, *2*) $Sm(Co,Fe,Zr,Cu)_5$ phase, *3*) $Sm_2(Co,Fe,Zr,Cu)_7$ phase

SINTERING OF $Sm_2(Co,Fe,Zr,Cu)_{17}$ ALLOY POWDERS IN HYDROGEN

The study into the sintering conditions and characteristics for ferromagnetic Sm_2Co_{17}-based alloys at reduced temperatures in hydrogen commenced with analysis of properties peculiar to the microstructure of sintered materials depending on the grinding conditions, compaction pressure, and sintering stage. The stages are referred to as HD and DR. An industrial alloy doped with iron, zirconium, and copper to improve its properties was chosen for the study. Physical aspects of sintering for ferromagnetic materials at reduced temperatures involve hydrogen-induced phase transformations at 700–950°C. This process includes disproportionation (HD stage)—decomposition of the starting ferromagnetic phase into a metal hydride (in this case, $SmH_{2\pm x}$) and other phases—and recombination (DR stage)—decomposition of the hydride of a hydride-forming metal (in our case, Sm) to interact with other phases and create ferromagnetic phases present in the starting alloy. These transformations can be represented by the following scheme:

$$\text{Sm}_x(\text{Co,Fe,Cu,Zr})_y + \text{H}_2 \underset{\text{vacuum, } \approx 950^\circ\text{C}.}{\overset{\leq 1.5 \text{ MPa, } \approx 700^\circ\text{C}}{\leftrightarrow}} \text{SmH}_{2\pm x} + \text{Co(Fe,Cu,Zr)}$$

Further clarification should be provided for the disproportionation of the alloy under study as it consists of several ferromagnetic phases: primary $Sm_2(Co,Fe,Cu,Zr)_{17}$ phase, whose composition is predominant, along with $Sm(Co,Fe,Cu,Zr)_5$ and $Sm_2(Co,Fe,Cu,Zr)_7$ phases. Previous research [20] demonstrated that the $SmCo_5$-based alloy, also containing the Sm_2Co_7 phase, fully disproportionated into samarium hydride and cobalt/cobalt polymorphic modifications. In this two-phase alloy, the Sm_2Co_7 phase was the first to undergo disproportionation [21]. A comparison of these findings with the disproportionation conditions for the Sm_2Co_{17} phase [22] revealed that the stability of Sm–Co intermetallic phases in hydrogen increased as the REM content decreased. The substitution of cobalt with iron in samarium–cobalt compounds reduces the hydrogen pressure necessary for their disproportionation [23]. Consequently, when it is further stated in the paper that the $Sm_2(Co,Fe,Zr,Cu)_{17}$ alloy disproportionated, this implies that all phases present in the alloy underwent disproportionation.

SINTERING OF THE $Sm_2(Co,Fe,Zr,Cu)_{17}$ ALLOY GROUND AT $\nu = 100$ RPM FOR $\tau = 20$ AND 60 MIN IN HYDROGEN

Morphology of the $Sm_2(Co,Fe,Zr,Cu)_{17}$ Powder. Data are provided on the morphology of the ground alloy (Fig. 2) because the powder particle size influences the porosity of the sintered materials. Moreover, HDDR parameters depend on both the particle size and grain size in their microstructure. Powders ground at a frequency of 100 rpm for 20 and 60 min consist of particles with sizes that vary over a wide range, with their majority being approximately 100 μm (Fig. 2*a*). The coarse particles possess a refined microstructure with grain sizes ranging from 1 to 5 μm (Fig. 2*b*).

Microstructure of the $Sm_2(Co,Fe,Zr,Cu)_{17}$ Alloy Sintered through HD, with Powder Compaction Pressure of 2 and 5 t/cm^2, and through HDDR, with Compaction Pressure of 20 t/cm^2. A compaction pressure of 2 t/cm^2 was found to be inadequate for high-quality sintering of the alloy. Individual coarse particles sintered together, but the sintered material still contained pores with sizes up to 100 μm. After the compaction pressure was increased to 5 t/cm^2, the material sintered but was inhomogeneous in terms of both porosity and microstructure refinement (Fig. 3*a*). There were coarse (>100 μm) areas where the alloy sintered continuously, but there were also areas with cracks (Fig. 3*b*, areas *3*). The microstructure of the sintered material consisted of light and dark gray regions (Fig. 3*b*). The dark gray color belongs to the material where phase components disproportionated (Fig. 3*b*, area *2*), while the areas that did not undergo disproportionation appeared light gray (Fig. 3*b*, area *1*). The ferromagnetic $Sm_2(Co,Fe,Zr,Cu)_{17}$ phase is the main alloy component—this phase disproportionated only partially in coarse particles, because of their large sizes. In particular, a branched network of the disproportionated products was found on both sides (at ≈1 μm) of the grain boundaries present in the ground alloy particles (Fig. 3*c*). Fiber-like

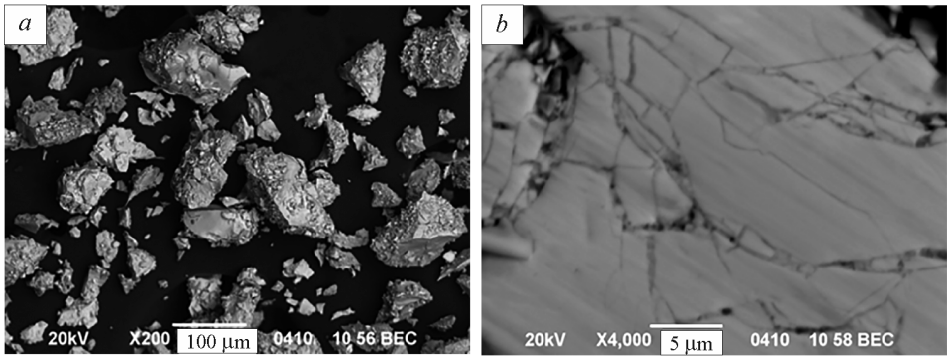

Fig. 2. Morphology (*a*) of the $Sm_2(Co,Fe,Zr,Cu)_{17}$ powder and particulate microstructure (*b*) of the $Sm_2(Co,Fe,Zr,Cu)_{17}$ alloy ground in hydrogen; ν = 100 rpm and τ = 20 min

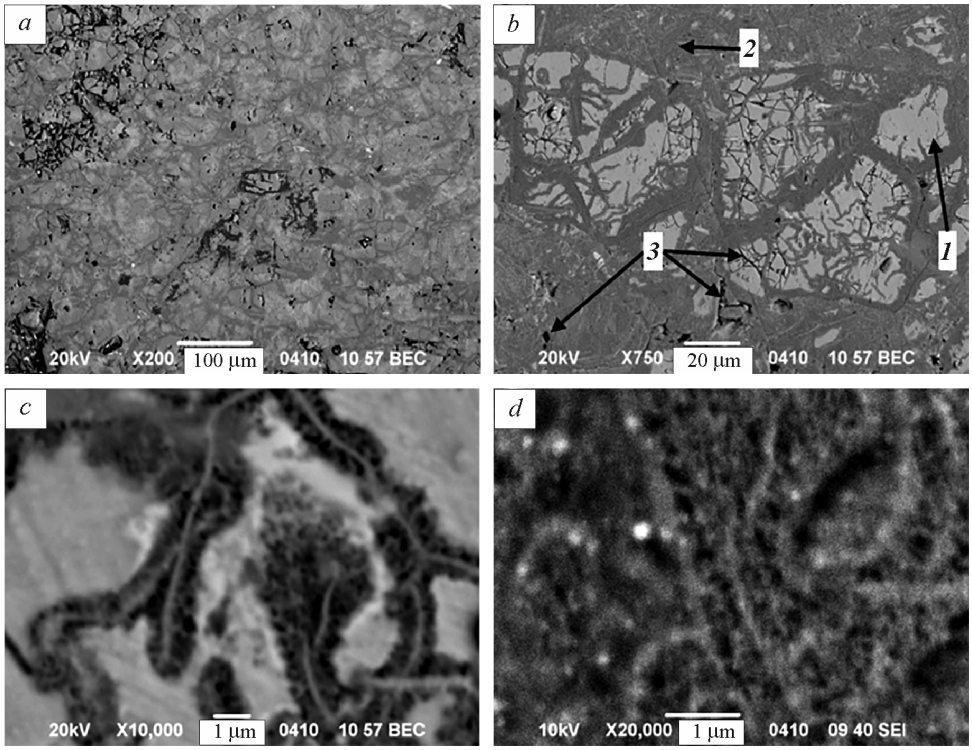

Fig. 3. Microstructure of the $Sm_2(Co,Fe,Zr,Cu)_{17}$ alloy sintered through HD; grinding at ν = 100 rpm for τ = 20 min; powder compaction pressure of 5 t/cm^2; HD hydrogen pressure of 1.5 MPa: *a*) unetched section; *b–d*) etched section; *1*) nondisproportionated phases; *2*) disproportionation products; *3*) pores and cracks

precipitates with sizes ranging from 90 to 250 nm in size and with increased cobalt content emerged at the boundaries (Fig. 3*c*). The disproportionation products are superfine, with grain sizes ≤100 nm (Fig. 3*d*).

After the compaction pressure was increased to 20 t/cm^2, the compacts were sintered through HDDR. Coarse particles sintered together, but the porosity remained high (Fig. 4, areas *1* and *2*).

SINTERING OF THE $Sm_2(Co,Fe,Zr,Cu)_{17}$ ALLOY GROUND AT ν = 200 RPM FOR τ = 60 MIN IN HYDROGEN

Morphology of the $Sm_2(Co,Fe,Zr,Cu)_{17}$ Alloy Powder. The hydrogenated $Sm_2(Co,Fe,Zr,Cu)_{17}$ alloy ground in a planetary-ball mill in hydrogen at ν = 200 rpm for 60 min decomposed into a powder with particle sizes ranging from ≈80 (Fig. 5*a*) to ≈0.5 μm (Fig. 5*b*). Numerous agglomerates were revealed in the powder. The

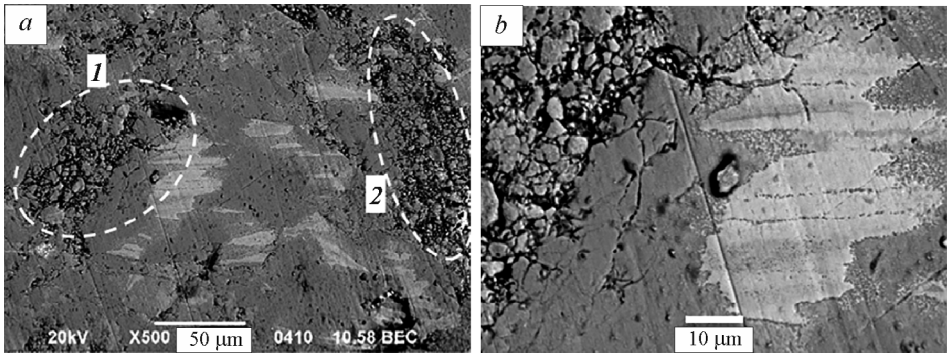

Fig. 4. Microstructure of the $Sm_2(Co, Fe, Zr, Cu)_{17}$ alloy sintered through HDDR; grinding conditions: ν = 100 rpm and τ = 60 min; powder compaction pressure of 20 t/cm^2; *b*) enlarged image of area *1* in Fig. *a*

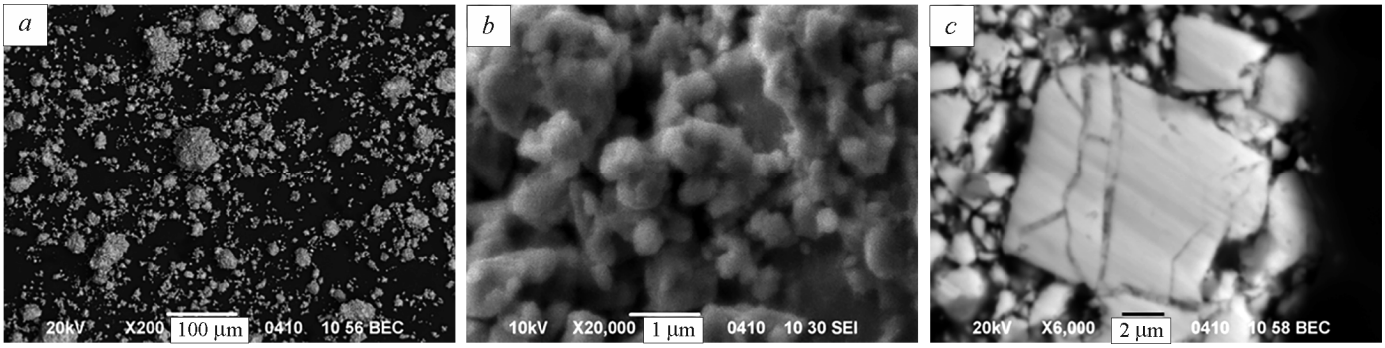

Fig. 5. Morphology (*a*, *b*) of the $Sm_2(Co,Fe,Zr,Cu)_{17}$ alloy powder and microstructure (*c*) of its particles; grinding conditions: ν = 200 rpm and τ = 60 min

agglomerates form when fine particles (from 2–3 μm to <0.5 μm) adhere to coarse ones (20–30 μm) (Fig. 5*b*). The coarse particles exhibit a fragmented microstructure with 2–3 μm grains (Fig. 5*c*).

Microstructure of the $Sm_2(Co,Fe,Zr,Cu)_{17}$ Alloy Sintered through HD; Compaction Pressure of 2 t/cm^2. The powder was compacted at a pressure of 2 t/cm^2 and sintered through HD. During sintering, the hydrogen pressure was 1.0 MPa and temperature was 700°C. The particles sintered together, but the material still had numerous pores and cracks (Fig. 6*a*, black areas 3). The microstructure of the coarse particles (≥10 μm) was inhomogeneous (Fig. 6*a,* areas *1* and *2*)). This inhomogeneity results from the disproportionation that occurs in the

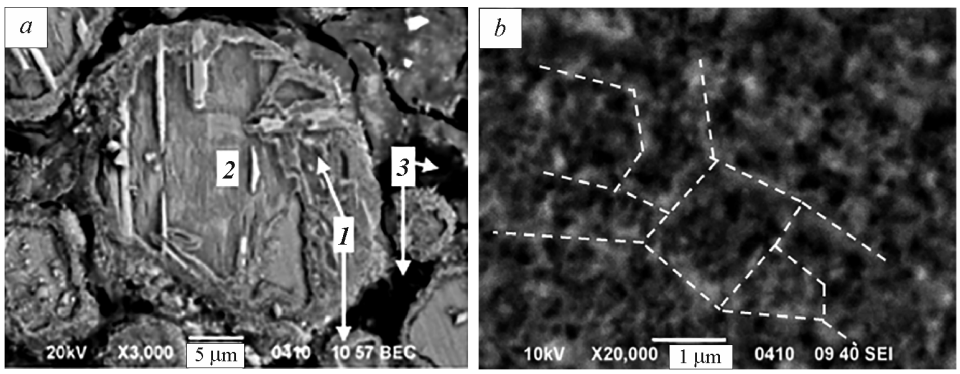

Fig. 6. Microstructure of the $Sm_2(Co,Fe,Zr,Cu)_{17}$ alloy sintered through HD; grinding conditions: ν = = 200 rpm and τ = 60 min; powder compaction pressure of 2 t/cm^2 (*a*): *1)* disproportionated area of particles; *2*) partially disproportionated particle; *3*) pores; dashed lines denote cell sizes of disproportionated products (*b*)

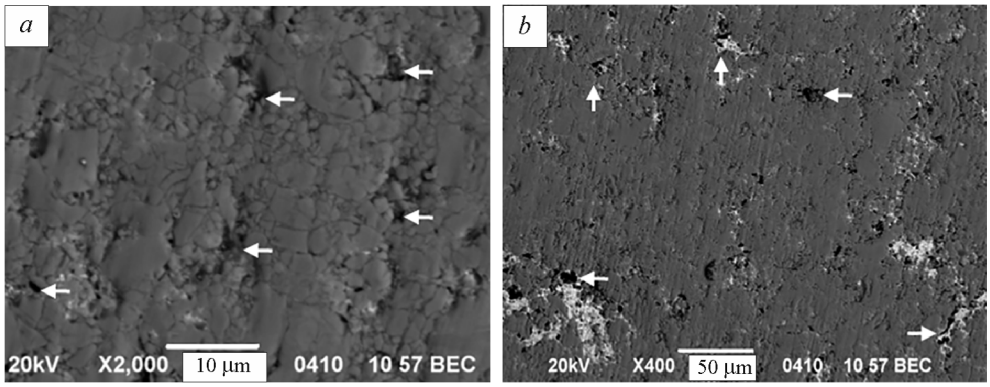

Fig. 7. Microstructure of the $Sm_2(Co,Fe,Zr,Cu)_{17}$ alloy sintered through HDDR: grinding at ν = = 200 rpm for τ = 60 min; powder compaction pressure of 2 t/cm^2; arrows point to pores

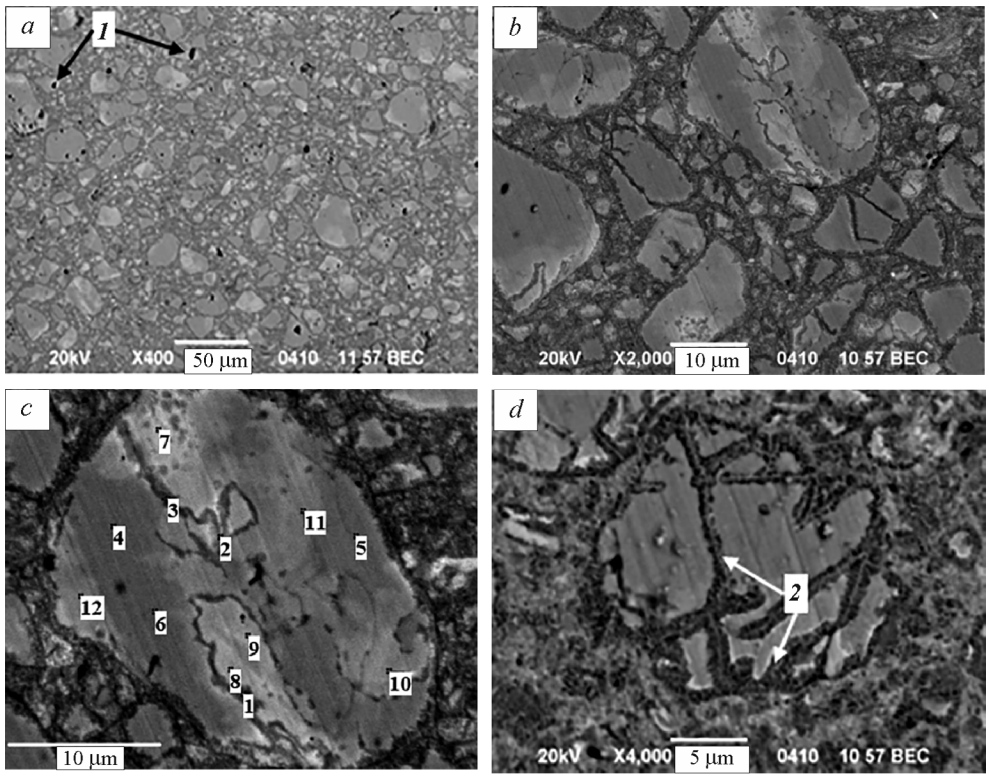

Fig. 8. Microstructure of the $Sm_2(Co,Fe,Zr,Cu)_{17}$ alloy sintered through solid HD: grinding at ν = = 200 rpm for τ = 60 min; powder compaction pressure of 5 t/cm^2; hydrogen pressure of 1.0 MPa and HD temperature of 700°C; unetched section (*a–c*); etched section (*d*); *1*) pores; *2*) areas with disproportionation products in coarse particles

TABLE 1. Content of Elements (at. %) in Different Areas of the Sintered Material (Fig. 8*c*)

Analysis area	Fe	Co	Cu	Zr	Sm
4–6	22.1–22.9	60.7–61.7	4.9–5.8	1.3–1.6	9.6–9.8
7–9	15.2–17.5	53.8–55.2	11.8–13.6	1.1–4.9	13.4–14.1
10–12	18.4–19.4	56.9–59.0	8.3–10.2	2.0–2.2	11.4–13.0

near-surface regions of the particles and at grain boundaries (Fig. 6*a*, area *1*). The morphology of the disproportionation products is characterized by a cellular structure, with the cells containing superfine grains (Fig. 6*b*). The cell walls are ≥1 μm in size, and their boundaries vary from 150 to 170 nm in width. The grain sizes inside the cells vary from 85 to 115 nm.

Microstructure of the $Sm_2(Co,Fe,Zr,Cu)_{17}$ Alloy Sintered through HDDR; Compaction Pressure of 2 and 5 t/cm². Following HD in the conditions described above, the material was subjected to recombination (DR) at 950°C. The microstructure of the sintered material shows that its porosity is lower than that after sintering in HD conditions (Fig. 7).

The powder was compacted at 5 t/cm² and sintered in hydrogen through HD under 1.0 MPa at 700°C. The material sintered well, and the number of pores was low (Fig. 8*a*, points *1*). The coarse powder particles (10–30 μm) were surrounded by fine ones (Fig. 8*b*). Elemental analysis revealed the main phases formed in alloys of this type (Fig. 8*c*; Table 1): $Sm_2(Co,Fe,Cu,Zr)_{17}$ (areas 4–6), $Sm(Co,Fe,Cu,Zr)_5$ (areas 7–9), and $Sm(Co,Fe,Cu,Zr)_7$ (areas 10–12). The coarse particles only began to disproportionate (Fig. 8*d*, area *2*). The HD products refined to the nanoscale (~70–110 nm grains).

Microstructure of the $Sm_2(Co,Fe,Zr,Cu)_{17}$ Alloy Sintered through HDDR, Compaction Pressure of 5 t/cm², and through DR at 950°C. The powder sintered well; superfine particles crumbled away in the preparation of sections (Fig. 9*a*). The coarse particles were surrounded by the fine ones (Fig. 9*b*). The material contained

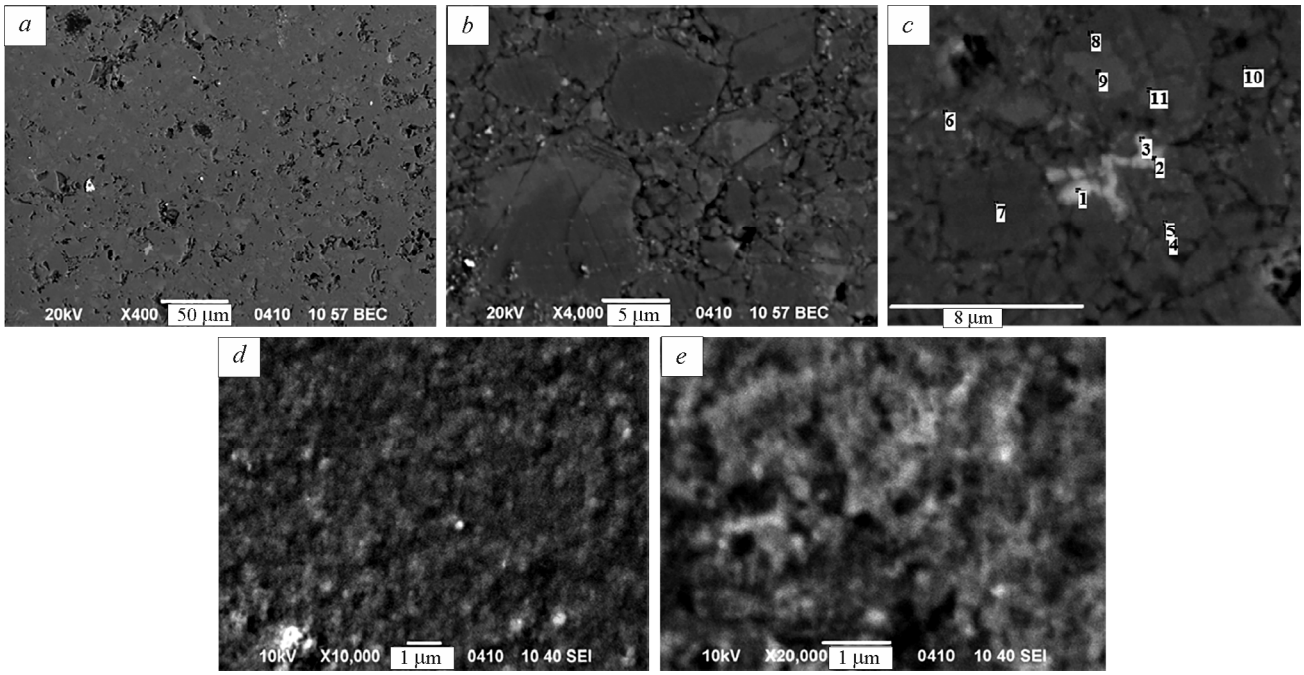

Fig. 9. Microstructure of the $Sm_2(Co,Fe,Zr,Cu)_{17}$ alloy sintered through HDDR: grinding at ν = = 200 rpm for τ = 60 min; powder compaction pressure of 5 t/cm²; hydrogen pressure of 1.0 MPa and HD temperature of 700°C; DR temperature of 950°C; *a–c*) unetched section; *d*, *e*) etched section

TABLE 2. Content of Elements (at.%) in Different Areas of the Sintered Material (Fig. 9*c*)

Analysis area	Fe	Co	Cu	Zr	Sm
1–3	12.6–16.4	31.1–42.4	3.4–4.1	1.8–2.4	35.3–50.5
4–6	19.1–20.2	56.2–56.8	5.1–7.0	2.6–3.1	14.0–16.2
7, 8, 10	21.0–22.1	59.0–60.8	6.5–8.0	0.7–2.1	9.8–10.3
9, 11	11.3–11.6	46.2–48.4	24.9–26.9	1.4–1.4	13.7–14.2

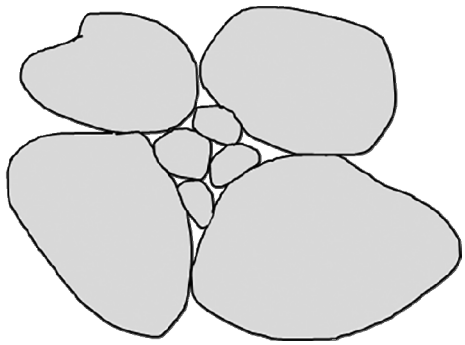

Fig. 10. Schematic arrangement of alloy particles in the compact

ferromagnetic $Sm_2(Co,Fe,Cu,Zr)_{17}$ and $Sm(Co,Fe,Cu,Zr)_5$ phases and samarium-rich regions (Fig. 9*c*; Table 2). The microstructure of the sintered alloy was refined. The phase grain sizes ranged from 100 to 220 nm (Fig. 9*d*) for $Sm(Co,Fe,Cu,Zr)_5$ and from 115 to 200 nm (Fig. 9*e*) for $Sm_2(Co,Fe,Cu,Zr)_{17}$.

DISCUSSION OF RESULTS

Analysis of High Porosity. Results from the lower-temperature sintering of ferromagnetic Sm_2Co_{17}-based alloy powders, produced by grinding at a frequency of 100 rpm, indicate the following. It was experimentally shown that the powders could sinter at the disproportionation stage at 700°C to form a mechanically integral material. However, these materials exhibit high porosity. The porosity does not decrease even when the compaction pressure increases by an order of magnitude (from 2 to 20 t/cm^2). Data on the morphology of the powders and on the microstructure of the sintered materials were used to build a schematic arrangement of the powder particles in the compact (Fig. 10). Coarse particles are located close to each other. The free space between them is filled with fine particles. A photograph of the powder (Fig. 2) indicates that the number of fine particles is small. Thus, their volume is insufficient to fully occupy the space between the coarse particles. For this reason, the materials are highly porous. The porosity of the sintered materials decreases when the powder particles are refined (Fig. 5) and compaction pressure of up to 5 t/cm^2 is applied (Fig. 8). The superfine (several microns) fraction of the powders is sintered (Fig. 3*b* and Fig. 8*b*). In the light of these findings, it can be suggested that homogeneous Sm_2Co_{17}-based alloy powders with particles of several microns in size can be sintered in hydrogen at lower temperatures and low-porosity superfine sintered magnets can be produced. It should be noted that such magnets will be anisotropic [24].

Analysis of Causes behind the Reduction in Sintering Temperature. The key sintering stages, particularly fusion and healing of pores or active sintering, are controlled by diffusion despite the diversity of their mechanisms [25, 26]. The diffusion rate for components in the material is important for determining the sintering conditions, such as temperature and time. The consideration of this fact in conjunction with the physical phenomena that transpire during sintering in hydrogen elucidates the rationale behind the reduction in sintering temperature.

The phenomena that occur during hydrogen treatment (disproportionation and recombination) account for both phase transformations and chemical reactions within a solid. These processes unfold through the diffusion of components [27, 28]. In each case, thermodynamic factors that trigger a transition of the alloy–hydrogen system to a state with lower energy are the driving force of the process. If the hydrogen pressure is high, the intermetallic is not thermodynamically stable and decomposes (disproportionates) into several phases. If the hydrogen pressure is low (vacuum), the hydride of a hydride-forming metal (in this case, REM) is thermodynamically unstable and disintegrates, while REM interacts with other phases to form the starting intermetallic. Hence, the diffusion of alloy components, which take place at relatively low temperatures during phase transformations (disproportionation/recombination), is a sufficient condition for particle sintering. Thus, if powders of the samarium–cobalt intermetallics, $SmCo_5$ and Sm_2Co_{17}, are heated to ≤1200°C to provide the energy necessary for diffusion (and hence for sintering) to their components, the required conditions (diffusion rate) can be achieved even at 700–950°C during disproportionation and recombination.

The second factor that contributes to the reduction in sintering temperature involves increase in the diffusion activity in metals/alloys as they form a solid solution of hydrogen [29]. The solid solution of hydrogen is present in the alloy during disproportionation and recombination. Before disproportionation, hydrogen penetrates into the alloy through grain boundaries to form a solid solution in it [30]. In the recombination process (DR), the metal hydride disintegrates, and hydrogen desorbs from the alloy by diffusion to form a solid solution once again.

The third factor that contributes to the reduction in sintering temperature is the size of material particles. According to metallographic studies, there is a superfine fraction (≈0.5 μm) in the powder. Literature data indicate that the sintering rate increases with the refinement of particles [25]. Furthermore, the 'overactivity' effect was noted in the sintering of powders with ≤0.1 μm (100 nm) particle sizes [26]. Consequently, the reduction in particle sizes to the micron level is accompanied by a decrease in the sintering temperature from 0.9 T_{melt} to 0.6–0.7 T_{melt}.

Other research findings, particularly those for titanium and its alloys [31], indicate that hydrogen-induced phase transformations are used to improve the sintering conditions and properties of the resulting materials. Although the latter case involves the disintegration of the titanium hydride phase during powder sintering, this does not alter the nature of physical phenomena, such as phase transformations and the presence of a solid solution of hydrogen, or their effect on sintering.

The first results from the sintering of ferromagnetic materials using the HDDR route were analyzed. The current issue with this method that needs attention is the inhomogeneity of microstructure refinement. This is caused by the wide distribution of particle sizes. Disproportionation is known to commence from the particle surface (when the material is in a powder state) or from the grain boundary, spreading toward the particle/grain center [30]. Both powder particles and grains of coarse polycrystalline particles differ in size by nearly an order of magnitude. As a result, the finest particles/grains undergo complete disproportionation, while the coarse ones only partial disproportionation. The microstructure is not refined in the alloy regions that did not undergo disproportionation. To increase the homogeneity of microstructure refinement, it is necessary, first, to homogenize the powder in terms of particle sizes and, second, to optimize the HD parameters (hydrogen pressure, temperature, reaction duration).

Process Advantages. The new method of sintering for ferromagnetic materials has process advantages over similar techniques described in the literature. In particular, the method does not require the material to be held at the highest heating temperature, as is the case in sintering at 970°C [32]. This process also takes place without the need for complex dies for extrusion or intricate equipment for spark plasma sintering. Simultaneously, HDDR produces anisotropic materials and thus holds the potential for the manufacture of anisotropic nanostructured sintered magnets.

CONCLUSIONS

The idea of potential reduction in the sintering temperature for Sm_2Co_{17}-based ferromagnetic alloy powders from ≤1200°C to 700–950°C using hydrogen as a working environment has been proposed and verified experimentally. The physical basis for this outcome is ascribed to an increase in the diffusion rate for alloy components, resulting from hydrogen-induced phase transformations and the presence of a solid solution of hydrogen in the alloys.

The features peculiar to the sintering of ferromagnetic materials in hydrogen through HD and HDDR have been studied. The experiments have shown that, in both cases, the powders are sintered at temperatures up to 950°C to form a mechanically integral material. The porosity of the sintered materials decreases as the powder particles are refined. The compaction pressure required for producing low-porosity sintered materials has been estimated to fall within the range of 2 to 5 t/cm^2.

Ways have been proposed to improve the microstructure of materials sintered at lower temperatures, specifically aiming to augment their homogeneity and decrease the porosity through optimizing the sintering parameters and homogenizing the powders in terms of particle sizes.

ACKNOWLEDGMENTS

The authors express their gratitude to Prof. M.S. Kovalchenko for the participation in discussion of the research results.

REFERENCES

1. O. Gutfleisch, M.A. Willard, E. Brück, C.H. Chen, S.G. Sankar, and J. Ping Liu, "Magnetic materials and devices for the 21st century: stronger, lighter, and more energy efficient," *Adv. Mater.*, **23**, 821–842 (2011).
2. *REN21. Renewables 2021 Global Status Report*, REN21 Secretariat, ISBN 978-3-9818107-0-7, Paris, www.ren21.net.
3. Y. Yang, A. Walton, R. Sheridan, K. Güth, R. Gauß, O. Gutfleisch, M. Buchert, B.-M. Steenari, T.V. Gerven, P.T. Jones, and K. Binnemans, "REE Recovery from end-of-life NdFeB permanent magnet scrap: a critical review," *J. Sustain. Metall.*, **3(1)**, 122–149 (2016).
4. J. Liu, "Some design considerations using permanent magnets," in: *Magnetics Magazine: Business and Technology*, March 13 (2016): https://magneticsmag.com/some-design-considerations-using-permanent-magnets.
5. J.M.D. Coey, "Perspective and prospects for rare earth permanent magnets," *Engineering*, **6(2)**, 119–131 (2019).
6. J. Liu, *Sm–Co Magnets and Applications*, International Magnetics Association, Electron Energy Corporation (2010): https://www.electronenergy.com/brochures-white-papers/; https://cdn2.hubspot.net/hubfs/4788906/Electronenergy_December2018/Docs/SmCo-Magnets-and-Applications.pdf.
7. E.F. Kneller and R. Hawing, "The exchange-spring magnets: a new material principle for permanent magnets," *IEEE Trans. Magn.*, **27**, 3588–3600 (1991).
8. H. Fukunaga and H. Nakamura, "Computer simulation of magnetic properties of anisotropic nanocomposite magnets," *IEEE Trans. Magn.*, **36(5)**, 3285–3287 (2000).
9. R. Skomski and J.M.D. Coey, "Giant energy product in nanostructured two-phase magnets," *Phys. Rev.*, 48, 15812–15816 (1993).
10. J.P. Liu, E. Fullerton, O. Gutfleisch, and D.J. Sellmyer, *Nanoscale Magnetic Materials and Applications*, Kyiv (2009), p. 719.
11. L. Zheng, B. Cui, L. Zhao, W. Li, and G.C. Hadjipanayis, "Sm_2Co_{17} nanoparticles synthesized by surfactant-assisted high energy ball milling," *J. Alloys Compd*., **539**, 69–73 (2012).
12. N. Lu, X. Song, X. Liu, and J. Zhang, "Preparation and magnetic properties of amorphous and nanocrystalline Sm_2Co_{17} alloys," *Intermetallics*, **18**, 1180–1184 (2010).
13. S. An, L. Zheng, T. Zhang, and C. Jiang, "Bulk anisotropic nanocrystalline $SmCo_{6.6}Ti_{0.4}$ permanent magnets," *Scr. Mater*., **68**, 432–435 (2013).
14. Z. Zhang, X. Song, and W. Xu, "Phase evolution and its effects on the magnetic performance of nanocrystalline $SmCo_7$ alloy," *Acta Mater*., **59**, 1808–1817 (2011).
15. M.Q. Huang, Z. Turgut, B. Wheeler, D. Lee, S. Liu, B.M. Ma, Y.G. Peng, S.Y. Chu, D.E. Laughlin, J.C. Horwath, and R.T. Fingers, "Fully dense anisotropic nanocomposite Sm $(Co,Fe,Zr,Cu,B)_z$, z = 7.5–12 magnets," *J. Appl. Phys*., **97**, 10H104-10H104-3 (2005).
16. A.M. Gabay, W.F. Li, and G.C. Hadjipanayis, "Effect of hot deformation on texture and magnetic properties of Sm–Co and Pr–Co alloys," *J. Magn. Magn. Mater.*, **323**, 2470–2473 (2011).
17. C. Rong, Y. Zhang, N. Poudyal, I. Szlufarska, R.J. Hebert, M.J. Kramer, and J. Ping Liu, "Self-nanoscaling of the soft magnetic phase in bulk SmCo/Fe nanocomposite magnets," *J. Mater. Sci*., **46**, 6065–6074 (2011).
18. *Electronic Register*, http://www.ccp14.ac.uk.
19. *Electronic Register*, http://www.ill.eu/sites/fullprof.

20. I.I. Bulyk, A.M. Trostyanchin, and V.I. Markovych, “Phase transformations in the $SmCo_5$-based alloy initiated by hydrogen at a pressure to 650 kPa,” *Fiz..-Khim. Mekh. Mater.*, No. 1, 94–98 (2007).
21. I.I. Bulyk, V.V. Burkhovetskii, and A.M. Trostyanchin, “Change in the phase and structural state of the $SmCo_5$-based alloy in solid HDDR at lower hydrogen pressure,” *Metallofiz. Noveisz. Tekhnol.*, No. 2, 169–184 (2015).
22. I.I. Bulyk and P.Ya. Lyutyy, “Effect of hydrogen pressure on Sm_2Co_{17} disproportionation,” *Metallofiz. Noveisz. Tekhnol.*, **35**, No. 9, 1283–1294 (2013).
23. I.I. Bulyk, M.V. Pilat, and P.Ya. Lyutyy, “Hydrogenation, disproportionation, desorption, and recombination in the $Sm_2Co_{17-x}Fe_x$–H_2 system (x = 3.9 and 5.95). X-ray diffraction,” *Powder Metall. Met. Ceram.*, **53**, No. 5–6, 343–352 (2014).
24. I.I. Bulyk, “Use of hydrogen for producing sintered anisotropic nanostructured magnets from rare-earth and transition metal alloys,” *Fiz.-Khim. Mekh. Mater.*, No. 6, 10–23 (2018).
25. Ya.E. Geguzin, *Physics of Sintering* [in Russian], Moscow (1984), p. 311.
26. V.V. Skorokhod and S.M. Solonin, *Physical and Metallurgical Fundamentals of Powder Sintering* [in Russian], Moscow (1984), p. 159.
27. N. Cannesan and I.R. Harris, “Aspects of NdFeB HDDR powders: fundamentals and processing,” in: G.C. Hadjipanayis (ed.), *Bonded Magnets, NATO Science Series: II. Mathematics, Physics and Chemistry*, Vol. 118 (2002), pp. 13–36.
28. “Kinetics and same general features of hydrogen induced diffusive phase transformations in $Nd_2Fe_{14}B$ type alloys,” in: *Progress in Hydrogen Treatment of Materials*, Donetsk–Coral Gables: Kassiopeya (2001), pp. 368–390.
29. V.I. Pokhmurskii and V.V. Fedorov, *Effect of Hydrogen on Diffusion Processes in Metals* [in Ukrainian], Moscow (1998), p. 206.
30. O. Gutfleisch and I.R. Harris, “Fundamental and practical aspects of the hydrogenation, disproportionation, desorption and recombination process,” *J. Phys. D: Appl. Phys*., **29**, 2255–2265 (1996).
31. D.G. Savvakin, M.M. Gumenyak, M.V. Matviychuk, and O.G. Molar, “Role of hydrogen in the sintering of titanium powders,” *Fiz.-Khim. Mekh. Mater.*, No. 1, 72–81 (2011).
32. J.W. Kim, S.H. Kim, S.Y. Song, and Y.D. Kim, “Nd–Fe–B permanent magnets fabricated by low temperature sintering process,” *J. Alloys Compd*., **551**, 180–184 (2013).